Video Article

Fluorescence-mediated Tomography for the Detection and Quantification of Macrophage-related Murine Intestinal Inflammation

Tobias M. Nowacki[1], Dominik Bettenworth[1], Markus Brückner[1], Friederike Cordes[1], Frank Lenze[1], Anne Becker[2], Moritz Wildgruber[2], Michel Eisenblätter[2]

[1]Department of Medicine B, University Hospital Münster

[2]Translational Research Imaging Center, Department of Clinical Radiology, University Hospital Münster

Correspondence to: Tobias M. Nowacki at Tobias.Nowacki@ukmuenster.de

URL: https://www.jove.com/video/55942
DOI: doi:10.3791/55942

Keywords: Medicine, Issue 130, Medicine, gastroenterology, *in vivo* imaging, diagnostic imaging, experimental colitis, dextran sulfate sodium colitis, inflammatory bowel disease, fluorescence imaging

Date Published: 12/15/2017

Citation: Nowacki, T.M., Bettenworth, D., Brückner, M., Cordes, F., Lenze, F., Becker, A., Wildgruber, M., Eisenblätter, M. Fluorescence-mediated Tomography for the Detection and Quantification of Macrophage-related Murine Intestinal Inflammation. *J. Vis. Exp.* (130), e55942, doi:10.3791/55942 (2017).

Abstract

Murine models of disease are indispensable to scientific research. However, many diagnostic tools such as endoscopy or tomographic imaging are not routinely employed in animal models. Conventional experimental readouts often rely on *post mortem* and *ex vivo* analyses, which prevent intra-individual follow-up examinations and increase the number of study animals needed. Fluorescence-mediated tomography enables the non-invasive, repetitive, quantitative, three-dimensional assessment of fluorescent probes. It is highly sensitive and permits the use of molecular makers, which allows for the specific detection and characterization of distinct molecular targets. In particular, targeted probes represent an innovative tool for analyzing gene activation and protein expression in inflammation, autoimmune disease, infection, vascular disease, cell migration, tumorigenesis, *etc*. In this article, we provide step-by-step instructions on this sophisticated imaging technology for the *in vivo* detection and characterization of inflammation (*i.e.,* F4/80-positive macrophage infiltration) in a widely used murine model of intestinal inflammation. This technique might also be used in other research areas, such as immune cell or stem cell tracking.

Video Link

The video component of this article can be found at https://www.jove.com/video/55942/

Introduction

Animal models are widely used in scientific research, and many non-invasive procedures exist to monitor disease activity and vitality, such as the quantification of body weight changes or the analysis of blood, urine, and feces. However, these are only indirect surrogate parameters that are also subject to inter-individual variability. They must frequently be complemented by *post mortem* analyses of tissue specimen, which prevents serial observation at repetitive time points and direct observation of physiological or pathological processes *in vivo*. Sophisticated small-animal imaging techniques have emerged, including cross sectional imaging, optical imaging, and endoscopy, which enables the direct visualization of these processes and also allows for repetitive analyses of the same animals[1,2,3]. Additionally, the possibility to repetitively monitor various states of disease in the same animal might decrease the number of animals needed, which might be desirable from an animal ethics point of view.

Several different optical imaging techniques exist for *in vivo* fluorescence imaging. Originally, confocal imaging was employed to study surface and subsurface fluorescent events[4,5]. Recently, however, tomographic systems that allow for quantitative three-dimensional tissue assessments have been developed[6]. This has been accomplished through the development of fluorescent probes that emit light in the near-infrared (NIR) spectrum, offering low absorption, sensitive detectors, and monochromatic light sources[7]. While traditional cross-sectioning imaging techniques, such as computed tomography (CT), magnetic resonance imaging (MRI), or ultrasound (US), rely mostly on physical parameters and visualize morphology, optical imaging can provide additional information on underlying molecular processes using endogenous or exogenous fluorescent probes[8].

Advances in molecular biology have helped to facilitate the generation of smart and targeted fluorescent molecular probes for an increasing number of targets. For example, receptor-mediated uptake and distribution in a given target area can be visualized using carbocyanine derivative-labeled antibodies[9]. The abundance of available antibodies, which can be labeled to function as specific tracers in otherwise inaccessible areas of the body, provides unprecedented insights into molecular and cellular processes in models of tumorigenesis and neurodegenerative, cardiovascular, immunologic, and inflammatory diseases[7].

In this study, we describe the use of fluorescence-mediated tomography in a murine model of colitis. Dextran sodium sulfate (DSS)-induced colitis is a standard chemically induced mouse model of intestinal inflammation that resembles inflammatory bowel disease (IBD)[10]. It is particularly useful to assess the contribution of the innate immune system to the development of gut inflammation[11]. Since the recruitment, activation, and infiltration of monocytes and macrophages represent crucial steps in the pathogenesis of IBD, visualization of their recruitment

and the kinetics of infiltration are essential to monitoring, for example, the effect of potential therapeutic substances in a preclinical setting[12]. We describe the induction of DSS colitis and demonstrate the tomography-mediated characterization of macrophage infiltration into the gut mucosa using fluorescence molecular tomography for the specific visualization of the monocyte/macrophage marker F4/80[13]. Additionally, we illustrate auxiliary and supplemental procedures, such as antibody labelling; the experimental setup; and analysis and interpretation of the obtained images, in correlation with conventional readouts such as disease activity indices, flow cytometry and histological analysis, and immunohistochemistry. We discuss limitations of this technique and comparisons to other imaging modalities.

Protocol

All animal experiments were approved by the Landesamt für Natur, Umwelt und Verbraucherschutz (LANUV) Nordrhein-Westfalen according to the German Animal Protection Law (Tierschutzgesetz).

1. Materials and Experimental Setup

1. **Animal care.**
    1. Use sex- and age-matched mice of any DSS-susceptible strain (*e.g.,* C57BL/6) at 20-25 g bodyweight.
    2. Plan at least five or more mice per experimental group and house the mice according to local animal care guidelines.
    3. Provide a standard rodent chow diet and autoclaved drinking water *ad libitum*.
    4. Remove the standard chow and replace it with alfalfa-free chow at least three days prior to scanning to reduce endoluminal auto-fluorescence.

2. **Induction of acute DSS-induced colitis.**
    1. Dissolve 2 g of DSS (molecular weight ~40,000 Da) in 100 mL of autoclaved drinking water to obtain a 2% (w/v solution).
    2. Fill the drinking supply of the mice exclusively with the DSS solution and estimate 5 mL of liquid per mouse per day. Provide the same drinking water without DSS to the control mice[10].
    NOTE: Monitor the mice daily until the end of the experiment. Euthanize the mice that lose greater than 20% of their initial body weight or that become moribund (*i.e.,* persistently hunched posture, decreased movement, labored breathing, markedly erect coat) according to local applicable guidelines on animal welfare.

3. **Preparation of fluorescence-mediated tomography.**
    1. Label the desired antibody (*e.g.,* rat anti-mouse F4/80) with fluorescence dye (*e.g.,* Cyanine7, $\lambda_{excitation}$: 750 nm, $\lambda_{emission}$: 776 nm) as described in the manufacturer's protocol. Dialyze purified antibody in an appropriate dialysis membrane (pore size < 50-100 kDa) against 1 L of 0.15 M sodium chloride for at least 2 h or overnight.
        1. Transfer the antibody to 1 L of 0.1 M $NaHCO_3$ and dialyze for at least 2 h.
        2. Dissolve the required amount of fluorescent dye in dimethyl sulfoxide (DMSO) (10.8 µL/mg of antibody) and add it to the antibody solution. Use the fluorescent dye in 20-fold molar excess to achieve a dye-to-protein ratio of 1:3.
        3. Incubate in the dark at 4 °C for 1 h. Remove unlabeled antibody by dialysis against 1 L of 0.15 M sodium or by using a PD-10 desalting column and resolve in phosphate-buffered saline (PBS) for *in vivo* application.
        4. Determine the final antibody concentration and labeling ratio by spectrophotometry.
        5. Measure the protein concentration at an absorption of 250-330 nm and consider additional absorption by the dye. Correct the maximum absorption at 280 nm (protein) by 11% of the maximum absorption at 750 nm (next step) for Cyanine7 labeling.
        6. Measure a dilution of the compound (typically 1:10) at 250-800 nm and extract the concentration of Cyanine7 at 750 nm.
        7. Determine the dye-to-protein ratio as: dye/antibody = maximum absorption at 750 nm / 200,000 / (maximum absorption at 280 nm - 0.11 x max absorption at 750 nm) / 170,000.
        8. Keep the antibody solution at 4 °C and shield it from light to avoid bleaching before injection.
    2. Load the necessary antibody solution volume in a sterile syringe immediately before injection and shield from light until it is used.
    3. Determine the optimal timing of probe injection and the scanning procedure, depending on tracer pharmacokinetics.
    4. Anesthetize the mice using 1.5 - 2.5% inhaled isoflurane in oxygen or place them securely in a dedicated restrainer for the tail vein injection of the labeled antibodies .
    5. For full-length antibodies, inject the labeled antibody at least 24 h prior to scanning, such as for anti-mouse F4/80 macrophage visualization in murine colitis. Inject mice intravenously (i.v.) via the tail vein with labeled antibody in an amount corresponding to 2.0 nmol of dye .
    6. Use equally labeled unspecific antibodies (*e.g.,* rat IgG or another isotype corresponding to the primary antibody heritage) as an isotype control in doses equivalent to those of the specific probe.
    NOTE: The results of *in vivo* scans after injection of the control compound can serve as a reference for the interpretation of the specific probe imaging data.
    7. Use an electric razor to shave the animal fur in the abdominal region to minimize light reflection and absorption.

2. Technical Equipment

1. Use a veterinary fluorescence-mediated tomography (FMT) device for small-animal fluorescence (**Figure 4**).
2. Create a new study for each project by clicking the "new study" button and include in the study description the relevant tracers, including the imaging parameters and doses for future reference.
3. Within this study, create study groups according to the respective study design (*e.g.,* for the specific tracer and unspecific isotype control) by clicking the "new study group" button. Equip each study group with the respective number of animals.
4. Calibrate the system for the tracer constructs.

1. Perform the calibration for each batch of tracers to normalize for the variation in labeling and enable quantitative measurement from OI data.
2. Follow the instrument manufacturer's guidance for the calibration of each individual system; upon selection of "add new tracer," the system will provide a guide through the steps. Provide the dilution of the applied antibody solution and the calculated absolute concentration of tracer in the probe.
3. For FMT, use a tissue-mimicking phantom of defined thickness and absorption characteristics (resembling vital tissue) and fill it with a specific volume of the antibody solution used. Measure this on the FMT device.
   NOTE: The system will use the reference measurement of the provided probe, together with the given concentration, to calculate absolute tracer concentrations from future *in vivo* measurements.

5. Use a heatable examination cassette with a temperature of 42 °C.
   NOTE: This prevents the mice from becoming hypothermic during the examination.

3. Animal Anesthesia

1. Use a continuous flow of 1.5 - 2% vol% isoflurane ([2-chloro-2-(difluoromethoxy)-1,1,1-trifluoro-ethane]) and 1.5 L O_2/min to anesthetize the mice. Use specially designed inhalation systems for rodent anesthesia (isoflurane vaporizer) to easily control the anesthetic depth and to minimize staff exposure.
2. Place the mouse in the leak-proof induction chamber and turn on the vaporizer for isoflurane supply (100% (v/v), 5 vol% in oxygen, 3 L/min). Monitor the mouse until it is recumbent and unconscious.
3. Place it in the examination cassette for tomography, with continuous isoflurane inhalation via nose cone at a dose of 100% v/v, 1.5 vol% in oxygen, 1.5 L/min to minimize movement artefacts during examination. For procedures lasting longer than 5 min, apply eye ointment to the mouse eyes to prevent corneal damage.
4. Assess anesthetic depth by checking the reflexes. Lay the mouse on its back; if anesthesia is sufficient, the mouse should not turn around. Pinch the mouse softly between its toes; if anesthesia is sufficient, the leg will not be withdrawn (stage of surgical tolerance).

4. Fluorescence-mediated Tomography Scan

NOTE: Adapt the following details, which are specific to the FMT system used in this study (see the **Table of Materials**) for alternative fluorescence reflectance imaging devices or FMT systems, as needed.

1. Place the anesthetized mouse on its back in the examination cassette.
2. Perform the scanning procedure.
   1. Insert the cassette into the imaging system and close it immediately to ensure continuous anesthesia. Select the appropriate sample from the study group created previously. Select the administered tracer from the dropdown menu to ensure that the values for tracer concentration are properly calculated.
   2. Acquire fluorescence reflectance image at the appropriate wavelength (720 nm for Cyanine7) for scan planning and outline the scan field by clicking the "acquire image" button.
   3. See that the scan field appears as an overlay on the fluorescence reflectance image. Adjust it to the region of interest (*e.g.,* colon or abdomen), avoiding air or areas of remaining fur. Depending on the image target, set the number of image data points within the scan field by choosing from the coarse to medium and fine scan-field resolution in the menu on the right.
      NOTE: Keep in mind that a fine scan field might offer better spatial resolution at the cost of a significantly longer scanning time.
   4. Start data/image acquisition at the selected wavelength by clicking "scan."
      NOTE: The scan time for a medium-fine scan of the whole abdomen will be around 5 min; in this time, each data point is separately illuminated by the excitation laser, and the resulting fluorescence is recorded.
   5. Remove the animal from the imaging cassette at the end of the scan and allow the animal to recover entirely before placing it back into the cage.
   6. Repeat the FMT if deemed necessary at various time points during the experiment (*e.g.,* days 0, 5, and 9 - 10 (end of the experiment)), but consider the accumulation of antibody in the body, therefore increasing the background fluorescence signal.

5. Post-scan

1. Place the mouse in a separate cage on a paper towel under a red-light warming lamp and monitor the mouse for signs of discomfort or distress until full recovery. Place the mouse back into its respective cage when fully awake.
2. Euthanize the mice at the end of the experiment by the delivery of CO_2 to the isolator at a dose of 100% (v/v), 100 vol%, and 3 L/min. Do not pre-fill the chamber with CO_2, as a sudden exposure to high concentrations of CO_2 might cause distress. Verify death after the mouse has stopped breathing by a subsequent secondary mode of euthanasia such as rapid cervical dislocation.
3. Explant the colon by abdominal laparotomy and perform an *ex vivo* scan of the explanted colon, as explained in steps 4.2.1 - 4.2.4. Open each colon longitudinally using Metzenbaum surgical scissors and thoroughly rinse with saline solution before preparing it for further analysis.
4. Use a scalpel to cut a 0.5-cm fragment from the distal colon and immediately place it in a 1.5-mL cryogenic tube. Freeze it in liquid nitrogen and store at -70 °C until further use (*e.g.,*myeloperoxidase (MPO) measurements).
5. Use a wooden stick and roll up the remaining longitudinally opened colon from the distal to proximal end, with the mucosa outwards ("Swiss roll technique"), for histological analyses. Place the preparation in a fixative (see the **Table of Materials**) and freeze at -80 °C[14].

6. Data Reconstruction and Interpretation

1. Use the reconstruction tool of the respective imaging software to create 3D maps of the fluorescence distribution from the raw imaging data; scans are automatically added to the reconstruction tool, when upon scanning, the function "add to reconstruction queue" is selected.
    1. Otherwise, select the scans from the dropdown menu under the respective study and study group, right-click the scan, and select "add to reconstruction."

2. For further analysis, load a data set into the analysis software. From the dropdown menu in the top bar, select the respective study and then select the study group and the individual animal from the menu on the right; all scans performed for this animal will be shown. Select the correct scan and click "load."
   NOTE: The 3D reconstruction of the tracer distribution will appear on the left as an overlay of the initially acquired fluorescence reflectance image. The model can be rotated and magnified for easier analysis.
3. Identify foci of unspecific label accumulation (*e.g.,* liver or urine bladder) on reconstructed 3D maps and differentiate from target tissues (*e.g.,* bowel or intestine).
4. From the top bar, select the ROI shape most appropriate for the target. Label target tissue as regions of interest (ROI) by placing the respective measuring tools in the analysis software; the software will provide a fluorescence intensity for the ROI, as well as (pico-)molar amounts of the tracer that the scan has been calibrated for.
5. Select the total amount of tracer in the appropriate ROI, normalized for the ROI size, as the most suitable equivalent for the evaluation of disease activity in correlation with the inflammatory infiltrate (histology).
   NOTE: Other features of the ROI can be chosen if appropriate as representative of the particular model.

7. *Ex Vivo* Analyses

1. **Hematoxylin and eosin staining and immunofluorescence staining.**
    1. Deparaffinize sections by placing them in 70% ethanol (EtOH) for 2 min; rinse with distilled water afterwards. Stain with hematoxylin solution for 5 min and subsequently rinse with warm tap water for 10 min.
    2. Rinse with distilled water, counterstain with eosin solution for 2 min, and again rinse with distilled water.
    3. Place in 70% EtOH, 96% EtOH, 99% EtOH, and xylene (2 times) for 2 min each to dehydrate and clear the sections. Mount with resinous mounting medium.

2. **Immunofluorescence staining.**
    1. Use the previously obtained tissue sections ("Swiss roll") for immunofluorescence staining and prepare cryo-cut sections of 7 µm.
    2. Block acetone-fixed and frozen colon sections in 5.0% rat serum for 10 min and incubate overnight with diluted (1/500 v/v) biotinylated primary rat anti-mouse F4/80 antibody. Wash the sections thrice in Tris-buffered saline (TBS) and incubate with Streptavidin-FITC (1:100 v/v) in PBS/BSA (0.1% w/v) overnight at 4 °C.
    3. Wash the sections in TBS and stain with 4′,6-diamidino-2-phenylindole (DAPI, 1:1000 v/v) to achieve contrast. Analyze the fluorescence images under a confocal microscope (see the **Table of Materials**; 40x magnification; filter cube N2.1 with excitation filter 515 - 560) and count the F4/80-positive cells per high-power field.
       NOTE: Consider using antibodies of the same clone and format when combining *in vivo* FMT and *post mortem* histology analyses such as immunohistochemistry or immunofluorescence staining, depending on the intended target. For the detection of F4/80-positive macrophages *in vivo* and *ex vivo*, different formats were used.

3. **MPO measurements in colon samples.**
    1. Use freshly obtained, PBS-rinsed colon samples or thawed specimen for MPO measurements. Weigh all samples and homogenize the tissue in lysis buffer provided in the ELISA kit (see the **Table of Materials**) at a volume of 20 µL of lysis buffer per mg of tissue.
    2. Sonicate for 15 s (sonication frequency: 20 kHz, power: 70 W) and centrifuge the samples for 10 min at 200 x g and 4 °C.
    3. Use a commercially available ELISA kit (see the **Table of Materials**) according to the manufactures description. Carry out the test in duplicates.

Representative Results

Assessment of Colitis:

DSS-induced colitis is a chemically induced murine model of intestinal inflammation that resembles human IBD and leads to weight loss, rectal bleeding, superficial ulceration, and mucosal damage in susceptible mice[15]. It is particularly useful to study the contribution of the innate immune system to the development of intestinal inflammation[10,11]. To potently induce colitic inflammation, mice were continuously administered DSS throughout the experiment. Decreasing body weight and fecal occult blood were used as clinical indices of inflammation. As shown in **Figure 1A**, mice began losing weight starting at day four after the induction of colitis, whereas control animals receiving water alone showed no significant changes in body weight. In addition, colitic animals showed increased excretion of occult blood with feces (**Figure 1B**), as assessed using the following hemoccult scoring system: 0 (no blood), 1 (hemoccult positive), 2 (hemoccult positive and visual pellet bleeding), and 4 (gross bleeding, blood around anus)[16]. Colon length was measured to evaluate inflammation-induced colonic shortening, revealing significantly shortened colons in colitic mice as compared with control mice receiving water alone (**Figure 1C**). To directly assess colonic damage, histological analysis was performed at the end of the experiment. A quantitative assessment of histological damage was performed on colonic H&E-stained sections using an overall injury core based on the degree and extent of inflammation, crypt damage, and percent involvement[17]. Colitic mice showed signs of severe inflammation, while control mice receiving no DSS showed no histological damage (**Figure 1D**). The images demonstrate characteristic inflammatory changes in DSS-induced colitis, characterized by the destruction of epithelial architecture, with the loss of goblet cells, crypt damage, and mucosal ulceration, as opposed to the largely preserved mucosal architecture in control mice[18]. Statistical differences between the groups (n = 5 per group) were calculated by analysis of variance (ANOVA) followed by Student-Newman-Keuls (S.N.K.) *post hoc* test or by Welch's test followed by Games-Howell *post hoc* test in case of significant variance inhomogeneity. A *p*-value of < 0.05 was considered significant.

Assessment of Monocyte and Macrophage Recruitment:

As DSS-induced colitis is associated with the infiltration of immune cells, such as monocytes and macrophages, into the mucosa and submucosa of the colon, we used immunofluorescent staining for the monocyte/macrophage marker F4/80 to quantify the infiltrate. Colitic mice receiving DSS showed significantly elevated numbers of monocytes infiltrating the colon wall as compared to non-colitic control mice (**Figure 2A**). Leukocyte infiltration was additionally quantified using immunofluorescent staining for the neutrophil marker GR1, revealing the significantly increased immigration of neutrophils into the inflamed colon as compared to control mice (**Figure 2B**). To confirm, MPO levels reflecting both neutrophil number and inflammatory activity were significantly elevated in the colon tissue of colitic mice (**Figure 2C**). ANOVA and S.N.K. *post hoc* test were used to calculate the statistical significance between the groups (n = 5 per group). Statistical significance was set at $p < 0.05$.

Systemic Changes in Macrophage Subpopulation:

Mouse monocytes encompass a heterogeneous group of distinct subpopulations that differ in maturation state and their capacity to be recruited to inflammatory sites, where they participate in initiating and perpetuating the inflammatory response[19]. Therefore, we characterized blood monocytes by analyzing the differential expression of CD11b and Ly6C using flow cytometry. Under inflammatory conditions of acute DSS colitis, we observed a significant increase in inflammatory $CD11b^{high}Ly6C^{high}$ monocytes as compared to pre-experiment conditions. In contrast, this shift did not occur in non-colitic control mice without DSS (**Figure 3A**). The data (n = 5 per group) were analyzed using ANOVA and S.N.K. As an additional surrogate parameter for systemic inflammation, we assessed the presence of F4/80-positive cells in the spleen of colitic mice compared to non-colitic controls, which revealed a significant increase in DSS-treated mice (**Figure 3C**).

Fluorescence-mediated Tomography Scan:

We used fluorescence-mediated tomography to measure monocyte/macrophage recruitment and infiltration into the gut mucosa. A fluorescence-labeled antibody against murine F4/80 was employed to directly visualize activated macrophages in living animals. Labeled, unspecific rat IgG antibodies were used as the isotype control. For scanning, mice were shaved in the abdominal region to minimize light reflection by the fur, anesthetized by continuous isoflurane supply, and examined in a veterinary FMT device for small-animal fluorescence**.** As shown in **Figure 4A**, the induction of colitis led to a significantly elevated accumulation of fluorescent tracer in the colons of colitic mice as compared to non-colitic controls, indicating an increase in monocyte infiltration and differentiation into active macrophages in colitic animals. The application of an unspecific fluorescence-labeled IgG did not elicit a detectable fluorescence response in the abdomen and intestine, neither in the colitic (DSS) nor the non colitic (water) group, demonstrating the specificity of the probe-target interaction of the F4/80 antibody (**Figure 4A**). Representative images of the abdominal region are shown. The color code indicates the level of fluorescence intensity, which corresponds to the extent of inflammatory infiltrate**(Figure 4B** and **4C**). *Ex vivo* measurements of F4/80-directed tracer accumulation in explanted colons verified the colonic origin of the *in vivo* detected signal of F4/80 tracer accumulation (**Figure 5A** and **5B**). Calculated amounts of bound antibody correlated well ($R^2 = 0.52$) with histologically determined numbers of infiltrating macrophages (**Figure 5C** and **5D**), confirming that *in vivo* imaging with specific tracers can be indicative of local disease activity**.** Data were analyzed by ANOVA and S.N.K. *post hoc* test with a statistical significance level set at $p < 0.05$. The correlation was calculated as linear regression.

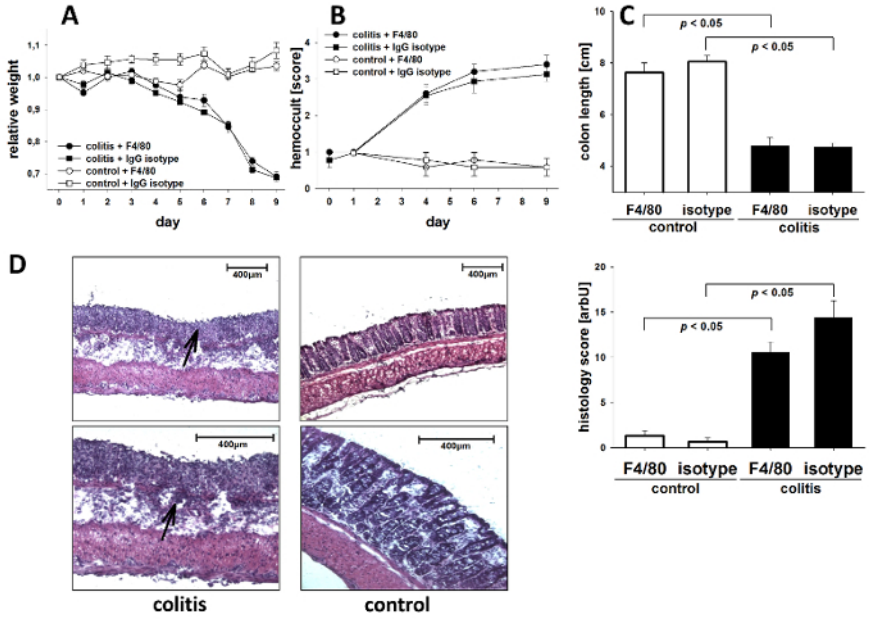

Figure 1. Clinical parameters and histological injury over the course of acute DSS colitis.
C57BL/6 mice were challenged with DSS (2% w/v) in drinking water for 8 days. Control mice were given drinking water without DSS. Animals were euthanized on day 9. Shown are data from one experiment (n = 5 per group) ± the standard error of the mean (SEM). **(A)** Changes in bodyweight are presented relative to the initial weight. **(B)** Blood excretion in feces, as determined by the guaiac paper test (hemoccult, 0 = negative, 4 = blood macroscopically). **(C)** *Post mortem* colon length. **(D)** Histological injury as assessed by the degree of crypt damage and the extent of inflammation. Shown are representative histological images (haematoxylin/eosin staining; magnifications: 10x (upper panel), 20x (lower panel)) of colitic (left panels) or control (right panels) mice. Note the profound destruction of epithelial architecture and inflammatory infiltrates (arrowheads). Bar graph: injury score. Please click here to view a larger version of this figure.

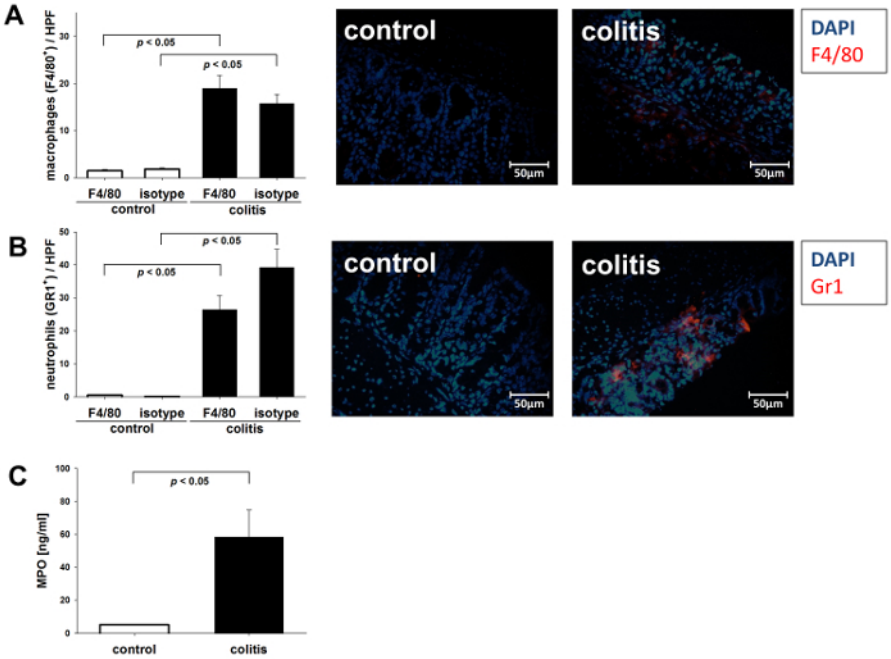

Figure 2. Intestinal monocyte and macrophage infiltrate.
DSS colitis was induced in C57BL/6 by the application of DSS (2% w/v) in the drinking water. Control mice received drinking water alone. The data from n = 5 mice per group are shown ± SEM. **(A)** Immunofluorescent visualization of macrophage infiltrations in the mucosa. Shown are representative images of anti-F4/80 staining in colitic and control mice. Bar graph: cell count/high power field (HPF). **(B)** Immunofluorescent visualization of mucosa neutrophil infiltrations. Shown are representative images of anti-Gr-1 staining in colitic animals and controls. Bar graph: cell count/HPF. **(C)** MPO concentration in the colonic tissue of colitic and non-colitic mice. Please click here to view a larger version of this figure.

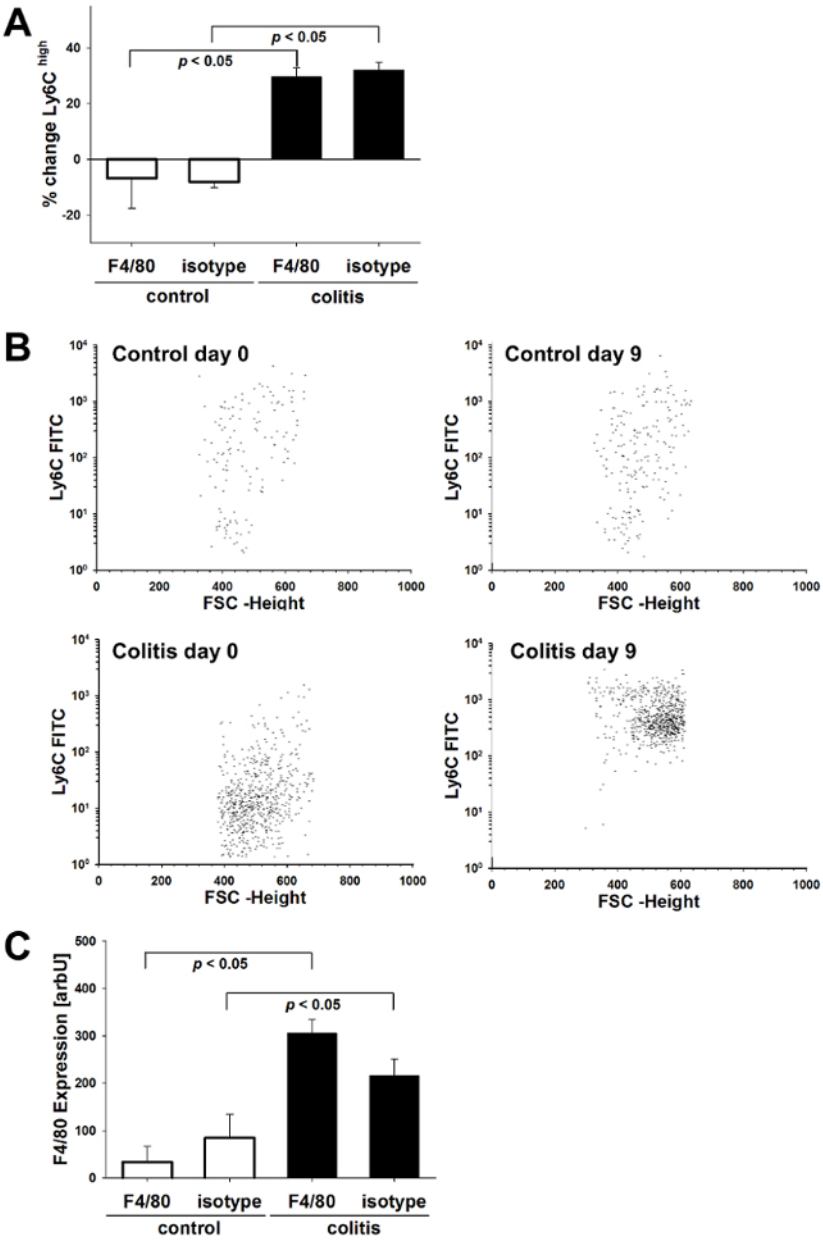

Figure 3. Monocyte recruitment to the intestinal compartment.
Peripheral blood monocytes from colitic mice as well as control mice (n = 5 per group) were analyzed by flow cytometry for the expression of Ly-6C on CD11b-positive cells. Cells were sorted based on SSC and CD11b expression. Mouse monocytes were identified as $SSC^{low}CD11b^{high}$ cells, and their Ly6C expression was analyzed. **(A)** Proportional changes towards inflammatory $Ly6C^{high}$ monocytes are depicted relative to pre-experiment conditions (% change ± SEM). **(B)** FACS dot plots of Ly6C expression on $SSCl^{ow}CD11b^{high}$ cells of colitic animals before and after colitis induction (lower panels) and controls pre- and post-experiment (upper panels). **(C)** Splenocytes from colitic and non-colitic mice were assessed for the expression of F4/80 by flow cytometry (mean fluorescence intensity ± SEM). Please click here to view a larger version of this figure.

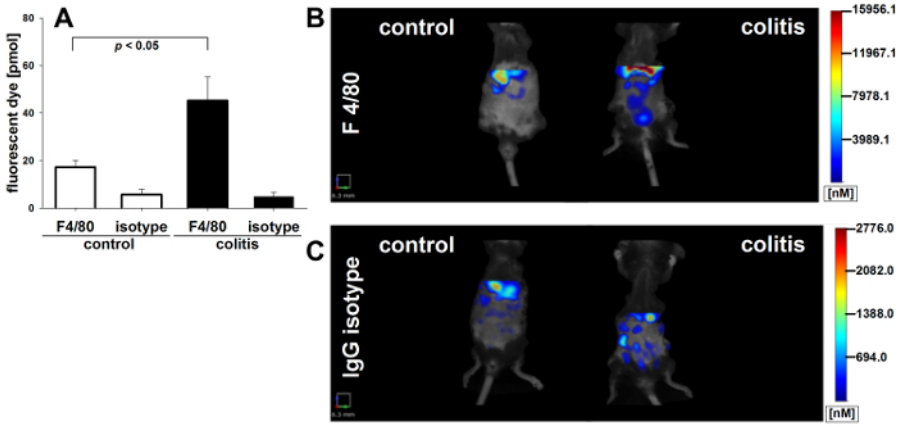

Figure 4. Tomographic visualization of macrophage infiltrate in murine colitis.
FMT scans in colitic mice and non colitic controls administered Cyanine7-conjugated antibody against murine F4/80 (n = 5 per group). **(A)** Bar graph: total fluorescence intensity in pmol of dye was determined in the ROI and depicted ± SEM. Representative images are shown with color-coded fluorescence intensity corresponding to the extent of inflammatory infiltrate in mice injected with the specific probe (anti-mouse F4/80) **(B)** and an unspecific control (rat IgG) **(C)**. In both cases, an ROI of equal size was placed transverse in the upper abdomen for further analysis. Please click here to view a larger version of this figure.

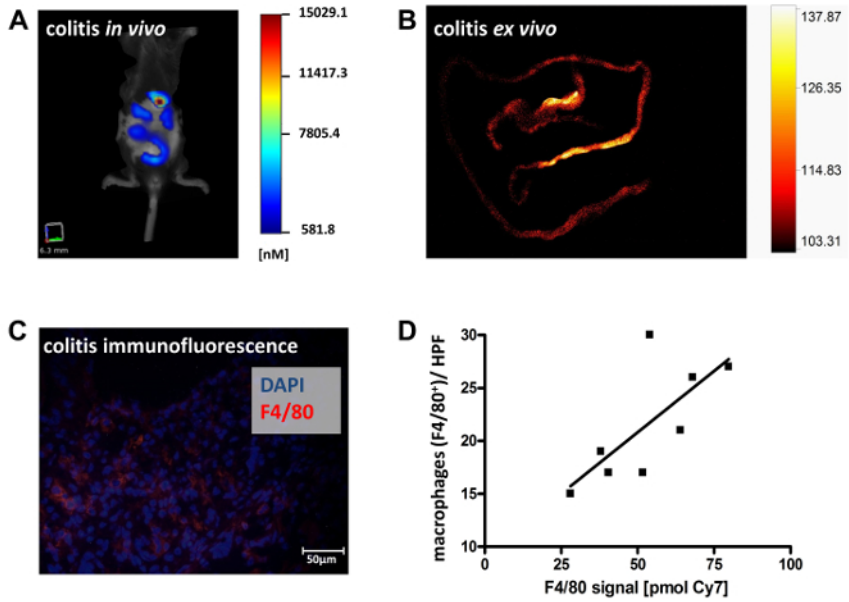

Figure 5. *Ex vivo* validation of tracer specificity in murine colitis.
In vivo FMT scans in colitic mice injected with the specific probe (anti-mouse F4/80) were followed by *ex vivo* planar fluorescence scans of explanted intestines to demonstrate the colonic origin of the tracer signal obtained *in vivo.* Data from two experiments with a total of n = 8 animals are shown. Representative images are shown depicting *in vivo* FMT scans of colitic mice with color-coded fluorescence intensity corresponding to the extent of inflammatory infiltrate **(A).** Fluorescence reflectance imaging of the explanted bowel allows for the identification of specific regions with tracer accumulation **(B).** Representative *post mortem* immunofluorescent staining for F4/80-positive macrophages from such areas confirms the *in vivo* results **(C).** The number of infiltrating macrophages, as determined by immunofluorescence staining, were correlated with *in vivo* measured tracer accumulation **(D).** Please click here to view a larger version of this figure.

Discussion

Although medical imaging techniques have evolved rapidly in recent years, we are still limited in our ability to detect inflammatory processes or tumors, as well as other diseases, in their earliest stages of development. However, this is crucial to understanding tumor growth, invasion, or metastases development and cellular processes in the development of inflammatory disorders and degenerative, cardiovascular and immunological diseases. While traditional imaging techniques rely on physical or physiological parameters, molecular imaging enables the visualization of specific molecular markers *in vivo*[20].

For small-animal imaging, radionuclide-driven approaches (*e.g., s*ingle-photon emission computed tomography (SPECT) and positron emission tomography (PET)), ultrasound, and fluorescence-mediated imaging can be used to visualize specific molecular target structures. The use of

full-length antibodies as the most available tracer backbone requires long-lasting labels, as long circulation times and slow tissue penetration delay the time of imaging after tracer application. Typical imaging radionuclides are therefore not suitable for the *in vivo* imaging of antibody distribution. The use of long-living isotopes like Cu64 or In111 enables antibody-based tracers but demands a complex infrastructure spanning isotope generation, radiation safety before and during the labeling procedure, and shielded animal housing after probe application. The more cost-effective and safer variant would be fluorescence-mediated imaging.

Several *in vivo* imaging systems for the detection, visualization, and measurement of fluorescent dye distribution in living animals have been presented over the past two decades[21]. Most systems enable rapid planar imaging suitable for superficial lesion imaging. Due to light absorption and scattering, signals deep in the tissue evade planar imaging. The most prominent solution for this problem is fluorescence tomography[22]. Based on mathematical modeling, the image signal is corrected for scattering and light absorption and a virtual 3D dataset is calculated from the multi-projection dataset[8]. The algorithm provides fully quantitative data, enabling the estimation of the tracer concentration in specific regions representative of the target concentration/expression[23]. A relevant limitation of FMT is related to poor spatial resolution as compared to anatomical imaging techniques, which might-depending on the desired target-compromise the allocation of molecular information to specific anatomical structures. Another limitation lies in the restricted penetration depth of light into tissue, which requires the use of probes absorbing and fluorescing in the red to NIR spectral range[23].

A recently introduced imaging modality that combines the advantages of morphological ultrasound and the possibility of obtaining molecular information from fluorescence imaging is optoacoustic imaging. Preliminary results from early studies suggest that-despite a need for further technical refinement-optoacoustic imaging holds great promise for molecular imaging and potential translational applications[24].

The recruitment of leukocytes to the intestinal wall is a crucial step in the initiation and perpetuation of IBD, as is the recruitment of inflammatory cells to the site of infection or inflammation in many immune-mediated disease, such as autoimmune disease, infection, vascular disease, tumorigenesis, and many more[25]. As monocyte activation and infiltration into intestinal mucosa is an essential step in the pathogenesis of IBD, inhibition of monocyte infiltration, orchestrated by chemokines and integrin-cellular adhesion molecule interaction, is a promising therapeutic approach[12,26]. Therefore, monitoring leukocyte trafficking to the site of inflammation is crucial in the development of new therapeutic options to visualize the anti-inflammatory effects of the studied drugs. This may be of special interest because agents targeting leukocyte trafficking have been developed, and some anti-integrin antibodies are already available for IBD therapy, while further components will be available in the near future[26]. Vedolizumab, a humanized monoclonal antibody against the gut-specific α4β7 integrin subunit, and Etrolizumab, which binds the β7 subunit of the intestinal α4β7 and αEβ7 integrin heterodimers, have been approved[27,28]. Other agents (*e.g.,* the MAdCAM-1 PF-00547659 and sphingosine-1-phosphate (S1P) receptor modulators such as Ozanimod) are currently undergoing evaluation for the treatment of IBD[29,30].

When performing FMT, possible modifications of the technique include the selection of different tracer-target combinations, as well as combining FMT with structural imaging approaches to compensate for poor spatial resolution. A wide array of probe-target combinations has been established and commercialized. For specific projects, the labeling of custom antibodies can be done using commercial labeling kits and the above-described protocol. Depending on the antibody or smaller peptide chosen as the targeting moiety, commercial suppliers offer a wide array of different labels. Consider the desired dye, depending on the application: for deep-tissue imaging, a dye operating in the NIR spectrum (*e.g.,* Cy7, $\lambda_{ex/em}$ 750/780 nm) might be well-suited, while the overall brightness and effective light supply of dyes operating in the near-visible range of the spectrum (*e.g.,* GFP analogues) might be preferable. Virtually all dyes can be obtained as an active ester to label the lysine- residues of proteins, as well as with alternative binding moieties, such as maleimides for cysteine binding or biotin for the labeling of proteins equipped with specific labeling tags[31]. The selection of the label does not change the principle protocol but merely requires slight modifications of the labeling procedure and is important for a good imaging result. Another attractive modification to overcome the limitations in spatial resolution is to combine FMT with CT or MRI, enabling the annotation of anatomical structures with molecular information. The structural information can either be acquired sequentially as *a priori* information or simultaneously, which requires hybrid imaging instrumentation[32,33].

Certain steps of the protocol deserve special attention. As this technique can be adapted for a multitude of fluorescent photoprobes that target a variety of specific molecules representative of different molecular processes, it is essential to allow for the sufficient distribution of the probes and enrichment in the desired target region. The ideal time point for imaging might vary according to the probe-target combination. For example, antibody targeting of tumor receptors might be influenced by the diffusion rate to tumors, uptake and metabolism by the liver, and possible adverse immunogenic reactions[34]. Also consider relevant controls for specific imaging approaches. Specific tracers should always be validated against isotype controls reflecting perfusion effects and unspecific binding (*e.g.,* Fc receptor-mediated binding). Target-negative animals can serve as an additional control for tracer specificity, if such knockout models exist. Alternatively, blocking experiments can be performed to prove the specificity of antibody-target interactions[35].

The following are critical steps concerning the practicalities of the procedure: (1) Carefully determine the DSS concentrations used, as DSS susceptibility might vary between different mouse strains and manufactures/batches[36]. (2) Carefully select probe-target combinations. (3) Allow around 5 min of scan time for a sufficient scan of the whole abdomen. The optimal time point between tracer application and the imaging procedure needs to be carefully determined to allow for tracer accumulation in the desired target region. For intestinal F4/80 detection in murine colitis, the labeled antibody should be injected 24 h prior to scanning. (4) As unspecific label accumulation might occur (*e.g.,* in the liver), it is crucial to label the appropriate target tissue as ROI by placing the respective measuring tools. Moreover, sufficient controls for unspecific tracer distribution should be included-consider unspecific isotype controls to rule out perfusion effects and knockout or blocking studies to validate tracer-target interaction.

Typical sources of error related to the scanning procedure and data reconstruction include improper animal position, scan field, and exposure time. When positioning the animal, the fluorescing lesion should be surrounded by tissue on all sides to minimize reconstruction noise. Air bubbles trapped between the animal and the front glass plate of the imaging cassette might also increase noise and should be removed by moving the animal slightly. Over- or underexposure of the image can require a reacquisition scan with modified exposure settings, which can be found in the scan screen (reflectance image block: adjustments of the front LED intensity and exposure time). When combining *in vivo* antibody-based FMT measurements with *post mortem* histological analyses, such as immunohistochemistry or immunofluorescent staining, the use of antibodies of the same clone and format should be considered. Also, when performing repetitive FMT measurements in the same animals, the same formats and clones should be used to prevent possible cross-reactivity or the targeting of different epitopes.

Taken together, fluorescence mediated-molecular tomography enables the repetitive monitoring of the disease course and underlying pathophysiological processes. It can be applied to a plethora of biomedical studies and might be useful to accelerate drug testing or as an objective endpoint in individualized therapies. FMT-targeting of F4/80-expressing macrophages in models of inflammation provides a valuable noninvasive tool to visualize and quantify the infiltration and accumulation of inflammatory cells while also demonstrating good correlation to conventional readouts.

Disclosures

The authors have nothing to disclose.

Acknowledgements

We thank Ms. Sonja Dufentester, Ms. Elke Weber, and Mrs. Klaudia Niepagenkämper for the excellent technical assistance.

References

1. Bruckner, M. *et al.* Murine endoscopy for in vivo multimodal imaging of carcinogenesis and assessment of intestinal wound healing and inflammation. *J Vis Exp.* **90** (2014).
2. Lewis, J. S., Achilefu, S., Garbow, J. R., Laforest, R., Welch, M. J. Small animal imaging. current technology and perspectives for oncological imaging. *Eur J Cancer.* **38** (16), 2173-2188 (2002).
3. Bettenworth, D. *et al.* Translational 18F-FDG PET/CT imaging to monitor lesion activity in intestinal inflammation. *J Nucl Med.* **54** (5), 748-755 (2013).
4. Vowinkel, T. *et al.* Apolipoprotein A-IV inhibits experimental colitis. *J Clin Invest.* **114** (2), 260-269 (2004).
5. Korlach, J., Schwille, P., Webb, W. W., Feigenson, G. W. Characterization of lipid bilayer phases by confocal microscopy and fluorescence correlation spectroscopy. *Proc Natl Acad Sci USA.* **96** (15), 8461-8466 (1999).
6. Ntziachristos, V., Tung, C. H., Bremer, C., Weissleder, R. Fluorescence molecular tomography resolves protease activity in vivo. *Nat Med.* **8** (7), 757-760 (2002).
7. Ntziachristos, V., Bremer, C., Weissleder, R. Fluorescence imaging with near-infrared light: new technological advances that enable in vivo molecular imaging. *Eur Radiol.* **13** (1), 195-208 (2003).
8. Ntziachristos, V., Bremer, C., Graves, E. E., Ripoll, J., Weissleder, R. In vivo tomographic imaging of near-infrared fluorescent probes. *Mol Imaging.* **1** (2), 82-88 (2002).
9. Ballou, B. *et al.* Tumor labeling in vivo using cyanine-conjugated monoclonal antibodies. *Cancer Immunol Immunother.* **41** (4), 257-263 (1995).
10. Wirtz, S., Neufert, C., Weigmann, B., Neurath, M. F. Chemically induced mouse models of intestinal inflammation. *Nat Protoc.* **2** (3), 541-546 (2007).
11. Kawada, M., Arihiro, A., Mizoguchi, E. Insights from advances in research of chemically induced experimental models of human inflammatory bowel disease. *World J Gastroenterol.* **13** (42), 5581-5593 (2007).
12. Nowacki, T. M. *et al.* The 5A apolipoprotein A-I (apoA-I) mimetic peptide ameliorates experimental colitis by regulating monocyte infiltration. *Br J Pharmacol.* **173** (18), 2780-2792 (2016).
13. Hansch, A. *et al.* In vivo imaging of experimental arthritis with near-infrared fluorescence. *Arthritis Rheum.* **50** (3), 961-967 (2004).
14. Bialkowska, A. B., Ghaleb, A. M., Nandan, M. O., Yang, V. W. Improved Swiss-rolling Technique for Intestinal Tissue Preparation for Immunohistochemical and Immunofluorescent Analyses. *J Vis Exp.* **113** (2016).
15. Diaz-Granados, N., Howe, K., Lu, J., McKay, D. M. Dextran sulfate sodium-induced colonic histopathology, but not altered epithelial ion transport, is reduced by inhibition of phosphodiesterase activity. *Am J Pathol.* **156** (6), 2169-2177 (2000).
16. Kim, J. J., Shajib, M. S., Manocha, M. M., Khan, W. I. Investigating intestinal inflammation in DSS-induced model of IBD. *J Vis Exp.* **60** e3678 (2012).
17. Dieleman, L. A. *et al.* Chronic experimental colitis induced by dextran sulphate sodium (DSS) is characterized by Th1 and Th2 cytokines. *Clin Exp Immunol.* **114** (3), 385-391 (1998).
18. Kojouharoff, G. *et al.* Neutralization of tumour necrosis factor (TNF) but not of IL-1 reduces inflammation in chronic dextran sulphate sodium-induced colitis in mice. *Clin Exp Immunol.* **107** (2), 353-358 (1997).
19. Sunderkotter, C. *et al.* Subpopulations of mouse blood monocytes differ in maturation stage and inflammatory response. *J Immunol.* **172** (7), 4410-4417 (2004).
20. Willmann, J. K., van Bruggen, N., Dinkelborg, L. M., Gambhir, S. S. Molecular imaging in drug development. *Nat Rev Drug Discov.* **7** (7), 591-607 (2008).
21. Ntziachristos, V., Ripoll, J., Wang, L. V., Weissleder, R. Looking and listening to light: the evolution of whole-body photonic imaging. *Nat Biotechnol.* **23** (3), 313-320 (2005).
22. Ntziachristos, V. Going deeper than microscopy: the optical imaging frontier in biology. *Nat Methods.* **7** (8), 603-614 (2010).
23. Stuker, F., Ripoll, J., Rudin, M. Fluorescence molecular tomography: principles and potential for pharmaceutical research. *Pharmaceutics.* **3** (2), 229-274 (2011).
24. Beziere, N., Ntziachristos, V. Optoacoustic imaging: an emerging modality for the gastrointestinal tract. *Gastroenterology.* **141** (6), 1979-1985 (2011).
25. Habtezion, A., Nguyen, L. P., Hadeiba, H., Butcher, E. C. Leukocyte Trafficking to the Small Intestine and Colon. *Gastroenterology.* **150** (2), 340-354 (2016).
26. Ungar, B., Kopylov, U. Advances in the development of new biologics in inflammatory bowel disease. *Ann Gastroenterol.* **29** (3), 243-248 (2016).
27. Sandborn, W. J. *et al.* Vedolizumab as induction and maintenance therapy for Crohn's disease. *N Engl J Med.* **369** (8), 711-721 (2013).

28. Vermeire, S. *et al.* Etrolizumab as induction therapy for ulcerative colitis: a randomised, controlled, phase 2 trial. *Lancet.* **384** (9940), 309-318 (2014).
29. Coskun, M., Vermeire, S., Nielsen, O. H. Novel Targeted Therapies for Inflammatory Bowel Disease. *Trends Pharmacol Sci.* (2016).
30. Vermeire, S. *et al.* The mucosal addressin cell adhesion molecule antibody PF-00547,659 in ulcerative colitis: a randomised study. *Gut.* **60** (8), 1068-1075 (2011).
31. Terai, T., Nagano, T. Small-molecule fluorophores and fluorescent probes for bioimaging. *Pflugers Arch.* **465** (3), 347-359 (2013).
32. Ren, W. *et al.* Dynamic Measurement of Tumor Vascular Permeability and Perfusion using a Hybrid System for Simultaneous Magnetic Resonance and Fluorescence Imaging. *Mol Imaging Biol.* **18** (2), 191-200 (2016).
33. Ale, A., Ermolayev, V., Deliolanis, N. C., Ntziachristos, V. Fluorescence background subtraction technique for hybrid fluorescence molecular tomography/x-ray computed tomography imaging of a mouse model of early stage lung cancer. *J Biomed Opt.* **18** (5), 56006 1685476 (2013).
34. Chames, P., Van Regenmortel, M., Weiss, E., Baty, D. Therapeutic antibodies: successes, limitations and hopes for the future. *Br J Pharmacol.* **157** (2), 220-233 BPH190 (2009).
35. Faust, A., Hermann, S., Schafers, M., Holtke, C. Optical imaging probes and their potential contribution to radiotracer development. *Nuklearmedizin.* **55** (2), 51-62 (2016).
36. Mahler, M. *et al.* Differential susceptibility of inbred mouse strains to dextran sulfate sodium-induced colitis. *Am J Physiol.* **274** (3 Pt 1), G544-551 (1998).

